

# The Brain-Specific Beta4 Subunit Downregulates BK Channel Cell Surface Expression

Sonal Shruti<sup>1‡a</sup>, Joanna Urban-Ciecko<sup>1</sup>, James A. Fitzpatrick<sup>2‡b</sup>, Robert Brenner<sup>3</sup>, Marcel P. Bruchez<sup>2\*</sup>, Alison L. Barth<sup>1\*</sup>

**1** Department of Biological Sciences, Carnegie Mellon University, Pittsburgh, Pennsylvania, United States of America, **2** Molecular and Biosensor Imaging Center, Carnegie Mellon University, Pittsburgh, Pennsylvania, United States of America, **3** Department of Physiology, University of Texas Health Science Center at San Antonio, San Antonio, Texas, United States of America

## Abstract

The large-conductance K<sup>+</sup> channel (BK channel) can control neural excitability, and enhanced channel currents facilitate high firing rates in cortical neurons. The brain-specific auxiliary subunit  $\beta 4$  alters channel Ca<sup>++</sup>- and voltage-sensitivity, and  $\beta 4$  knock-out animals exhibit spontaneous seizures. Here we investigate  $\beta 4$ 's effect on BK channel trafficking to the plasma membrane. Using a novel genetic tag to track the cellular location of the pore-forming BK $\alpha$  subunit in living cells, we find that  $\beta 4$  expression profoundly reduces surface localization of BK channels via a C-terminal ER retention sequence. In hippocampal CA3 neurons from C57BL/6 mice with endogenously high  $\beta 4$  expression, whole-cell BK channel currents display none of the characteristic properties of BK $\alpha$ + $\beta 4$  channels observed in heterologous cells. Finally,  $\beta 4$  knock-out animals exhibit a 2.5-fold increase in whole-cell BK channel current, indicating that  $\beta 4$  also regulates current magnitude in vivo. Thus, we propose that a major function of the brain-specific  $\beta 4$  subunit in CA3 neurons is control of surface trafficking.

**Citation:** Shruti S, Urban-Ciecko J, Fitzpatrick JA, Brenner R, Bruchez MP, et al. (2012) The Brain-Specific Beta4 Subunit Downregulates BK Channel Cell Surface Expression. PLoS ONE 7(3): e33429. doi:10.1371/journal.pone.0033429

**Editor:** Stuart E. Dryer, University of Houston, United States of America

**Received:** November 8, 2011; **Accepted:** February 12, 2012; **Published:** March 16, 2012

**Copyright:** © 2012 Shruti et al. This is an open-access article distributed under the terms of the Creative Commons Attribution License, which permits unrestricted use, distribution, and reproduction in any medium, provided the original author and source are credited.

**Funding:** Work was supported by start-up funds from Carnegie Mellon University and National Institutes of Health (NIH) U54 RR022241. The funders had no role in study design, data collection and analysis, decision to publish, or preparation of the manuscript.

**Competing Interests:** The authors have declared that no competing interests exist.

\* E-mail: barth@cmu.edu (ALB); bruchez@cmu.edu (MPB)

‡a Current address: Biology Department, Brandeis University, Waltham, Massachusetts, United States of America

‡b Current address: Waitt Advanced Biophotonics Center, Salk Institute for Biological Studies, La Jolla, California, United States of America

## Introduction

The Ca<sup>++</sup>- and voltage-gated K<sup>+</sup> channel BK (maxiK, slo, KCMNA1), broadly expressed throughout the CNS, modulates firing and neurotransmitter release [1,2,3,4,5,6,7]. BK channel mutations have been associated with familial epilepsy [8,9], and BK channel antagonists can suppress cell-autonomous and network activity in vitro and prevent chemoconvulsant-induced seizures in vivo [4,7,10]. Furthermore, BK channel regulation has been linked to tolerance in alcoholism [11] and experience-dependent plasticity [12,13,14]. Thus, understanding the principles regulating BK channel function is relevant across many areas of contemporary neuroscience.

The BK channel is a tetramer of  $\alpha$  subunits [15,16] that assemble with an auxiliary  $\beta$  subunit in up to a 1:1 stoichiometry [17,18]. The four identified  $\beta$  subunit genes show tissue-specific expression (reviewed by [19]), where the most abundant CNS isoform is  $\beta 4$  [20,21]. Coexpression of  $\beta 4$  in heterologous cells slows activation kinetics of BK channel currents [20,22,23,24], generally increases the amount of Ca<sup>++</sup> and depolarization required for channel gating [21,23,25] but see [26], and confers resistance to the specific peptide antagonists iberio- and charybdotoxin [25,27]. Indeed, genetic knock-out of  $\beta 4$  results in larger BK channel currents gated by action potential (AP) firing and is associated with increased firing activity and spontaneous seizures in mice [1].

In contrast to the many investigations into how  $\beta 4$  influences the biophysical properties of BK channels, a role for this subunit in

controlling the cellular location of BK channels has not been systematically investigated [28], although other  $\beta$  subunits can modulate trafficking of the channel [29,30]. Regulated trafficking of BK channels in neurons is particularly interesting, as the number of endogenous channels at the plasma membrane may be small [31,32], in the tens to hundreds range, in contrast to Na<sup>+</sup> channels or glutamate receptors that are 100 to 1000-fold more densely distributed on the cell surface. Modest changes in the number of plasma membrane BK channels may profoundly influence the magnitude of whole-cell BK channel currents and, consequently, firing output and network excitability. Interestingly, although BK channels have been extensively studied in the CNS, few studies have detected BK channels with pharmacological or biophysical properties consistent with  $\beta 4$ -containing channels [20,21,22], despite the broad expression of this subunit across the brain.

To investigate the role of  $\beta 4$  in regulating cell-surface trafficking of BK channels, we used a novel fluorogen activating protein (FAP) [33] to genetically tag the extracellular N-terminus of the BK $\alpha$  subunit. Cotransfection of tagged BK $\alpha$  with  $\beta 4$  in HEK-293 cells led to a 70% reduction in cell-surface channel fluorescence, assessed by application of a membrane-impermeant dye. In the presence of  $\beta 4$ , BK $\alpha$  was sequestered in the ER, and mutation of a C-terminal ER retention/retrieval motif in  $\beta 4$  was sufficient to restore high levels of BK $\alpha$  at the plasma membrane.

How does  $\beta 4$  regulate BK channel currents in the CNS? Both BK $\alpha$  and  $\beta 4$  are highly expressed in CA3 pyramidal neurons.

However, whole-cell BK channel currents from CA3 neurons in wild-type mice do not appear to contain  $\beta 4$ , based upon their biophysical or pharmacological properties, consistent with a role for  $\beta 4$  in intracellular sequestration of the channel. Importantly, whole-cell BK channel currents in CA3 neurons from  $\beta 4$  knock-out mice are 2.5-fold larger than in wild-type or heterozygote animals. Taken together, our data indicate that the  $\beta 4$  subunit can regulate cell-surface BK channel localization.

## Materials and Methods

All animal experimental protocols were approved by Carnegie Mellon University's Institutional Animal Care and Use Committee (Animal welfare assurance number A3352-01).

### Cloning

Cortical and hippocampal tissues were collected from 3 C57BL/6 mice aged P14. RT-PCR was performed on RNA isolated from hippocampal tissue homogenates using gene-specific primers designed from annotated sequences (NCBI reference sequences NM\_010610.2 for KCNMA1/BK $\alpha$  and NM\_021452.1 for KCNMB4/ $\beta 4$ ), and PCR products were cloned and sequenced. The BK $\alpha$  variant isolated lacked the STREX exon. The  $\beta 4$  variant isolated was identical to published sequence (NM\_021452.1 for KCNMB4/ $\beta 4$ ). The L5 FAP was affinity-matured using published procedures (Szent-Gyorgi 2008), and a novel variant (L91S) with a 5-fold improved quantum yield was isolated. The L5-FAP was fused in-frame to the BK $\alpha$  sequence beginning at the amino acids MDAL at the N-terminus. The FAP-BK $\alpha$  construct was synthesized according to the RT-PCR-derived BK $\alpha$  sequence in a pUC57 vector (Genscript Corporation), and the BK $\alpha$  and  $\beta 4$  constructs were subcloned into the pCS2+ using a CMV promoter to drive expression in mammalian cells. Mutant  $\beta 4$  constructs were created by replacing C-terminal lysines in the last six amino acids to alanines for the  $\beta 4$ -Ala and by adding three serines to the C-terminal for the  $\beta 4$ -polySer construct.

### Cell culture and transfection

HEK-293FT (Invitrogen) cells were grown in complete DMEM medium with FBS at 37°C at 5% CO<sub>2</sub> and 75% humidity. Cells were seeded in 35 mm dishes and grown to ~70% confluence for 24 hours. HEK-293 cells were transfected using Neofectin (Mid Atlantic Biolabs) according to manufacturer's specifications. One  $\mu$ g BK $\alpha$  DNA was transfected, and an equimolar amount of  $\beta 4$  was included where indicated. Cells were cultured for another 24 hours post transfection and were either imaged live at 37°C in a humidified chamber or fixed for immunocytochemistry.

### Live-cell imaging and analysis

Images were acquired on a LSM 510 Meta confocal microscope (Carl Zeiss). Immediately before imaging, media was replaced with complete DMEM without FBS with either cell impermeable MG-2p (100 nM) or cell permeable MG-ester dyes (100 nM). Cells were maintained at 37°C, 5% CO<sub>2</sub> and 75% humidity throughout imaging. Fields for imaging and analysis were selected using only GFP fluorescence to identify transfected cells and were collected 3–10 minutes after dye addition.

Exported tiff files were analyzed in ImageJ. To determine surface fluorescence levels, mean cell membrane pixel intensities were determined as follows. A 250-pixel, circular ROI was placed on different regions of the plasma membrane of expressing cells (identified by both MG and GFP fluorescence) in a north-south-east-west orientation.

Because transient transfections with multiple plasmids does not guarantee expression of all plasmids (for example, some cells may not have taken up the  $\beta 4$  plasmid), analysis was limited to cells that exhibited both GFP fluorescence as well as MG-2P surface signal. This method may have led to an overestimation of surface localization of FAP-tagged BK $\alpha$  in the BK $\alpha$ + $\beta 4$  transfected cells, since some cells may not have expressed the  $\beta 4$  construct. Adjacent membranes from two transfected cells were rejected from analysis. ROIs for 2–4 cells were analyzed per image field, and 20 fields per transfection experiment were evaluated. Thus, ~60 cells per condition were examined for each experiment. Experiments were repeated at least three times. Mean, minimum and maximum pixel intensities for each ROI were calculated, averaged for each cell, and then averaged across cells for each separate transfection. To account for potential differences in expression levels across different transfection experiments, all transfection datasets were normalized to the value of the mean surface fluorescence for the BK $\alpha$ -alone transfection for that specific experimental day. A histogram for the normalized fluorescence intensity values across all experimental days was generated (see Figure 1).

### In situ hybridization

Digoxigenin (DIG)-labeled probes were prepared using the Roche DIG RNA Labeling Kit. The  $\beta 4$  probe isolated from our RT-PCR experiments spanned the entire transcript. Brains were collected from C57BL/6 animals of either sex, perfused with 4% paraformaldehyde (PFA) and fixed overnight in PFA. The tissue was sunk in 30% sucrose and sectioned at 50  $\mu$ m thickness on a cryostat. Sections were washed in PBS and MOPS buffer then placed in a hybridization solution overnight before incubating with the probe at 57°C for 5 days. Sections were then washed in MAB solution and blocked with 2% block (Roche) for 15 minutes at room temperature followed by overnight incubation with 1:2000 alkaline phosphatase conjugated anti-DIG antibody (Roche) in MAB+2% block. Hybridization signal was detected with an alkaline phosphatase reaction at 37°C for several hours.

### Immunocytochemistry and analysis

Twenty-four hrs post-transfection, HEK-293 cells were fixed in 4% PFA+4% sucrose for five minutes at room temperature. Cells were washed with PBS and permeabilized using a solution containing 0.5% Triton X-100, 5% 1 M glycine and 5% normal goat serum for 30 minutes at room temperature. Appropriate primary antibodies were diluted in this blocking solution and incubated with the transfected cells for 1 hour at room temperature. After washing with PBS, the cells were incubated with the appropriate secondary antibody for 30 minutes at room temperature. For experiments with non-permeabilized labeling, Triton X-100 was replaced with PBS in all solutions. Primary antibodies used were anti-BK $\alpha$  (Neuromab) and anti- $\beta 4$  (Neuromab for single labeling or Alomone labs for double-labeling) at a 1:500 dilution. Secondary antibodies used were Alexa 488-conjugated goat anti-rabbit (Invitrogen) 1:750, Alexa488-conjugated goat anti-mouse (Invitrogen) 1:750, Alexa594-conjugated goat anti-mouse (Invitrogen) 1:750 and Cy5-conjugated goat anti-mouse (Jackson Immuno Research) 1:750.

Quantitation of overlapping expression for BK $\alpha$  or  $\beta 4$  with KDEL-mRFP in fixed cells was done as follows. A line was drawn from the center of the nucleus to a point just outside the cell membrane, for portions of the plasma membrane that were not abutting another cell, and pixel intensities in both channels along this line were recorded for 10 cells from two separate transfections. For all cells the values for each channel were normalized to their

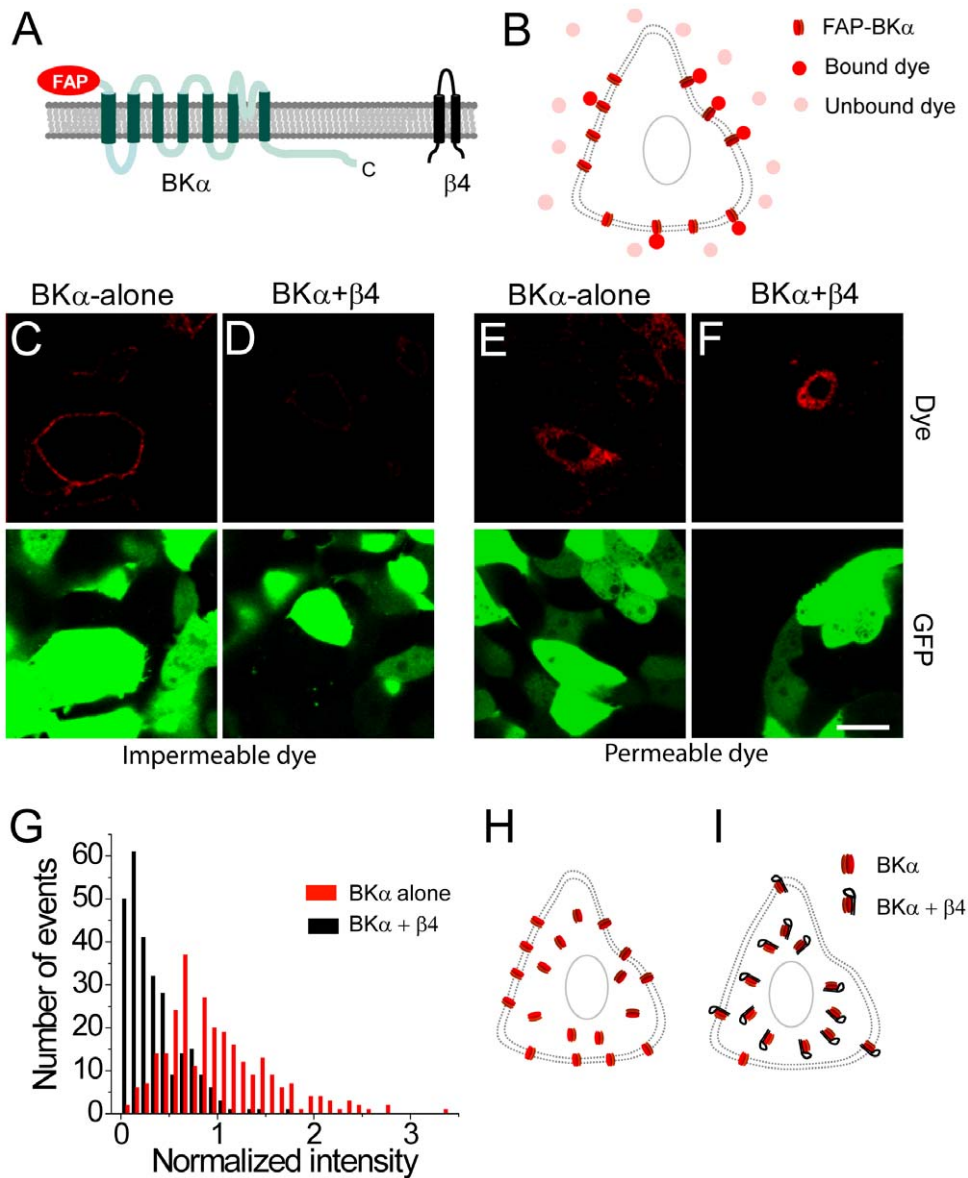


**Figure 1. Co-expression of the  $\beta$ 4 subunit reduces cell-surface trafficking of BK channels.** (A) Membrane topology of the FAP-BK $\alpha$  and  $\beta$ 4 proteins. The FAP tag is at the extracellular, N-terminus. The C-terminus of the BK $\alpha$  subunit is indicated. (B) Schematic of binding of cell-impermeable dye labels only surface BK $\alpha$  channels in live HEK-293 cells co-transfected with FAP-BK $\alpha$  (red) and GFP (green). (C) Application of cell-impermeable dye labels only surface BK $\alpha$  channels in live HEK-293 cells co-transfected with FAP-BK $\alpha$  (red) and GFP (green). (D) Same as (C) but in cells co-transfected with  $\beta$ 4, FAP-BK $\alpha$ , and GFP showing reduced surface expressed of the FAP-BK $\alpha$ . (E) Application of cell-permeable dye labels intracellular stores of channel in cells transfected with FAP-BK $\alpha$  (red) and GFP (green). (F) Same as (E) but in cells transfected with  $\beta$ 4, FAP-BK $\alpha$ , and GFP. Scale bar = 20  $\mu$ m (C-F). (G) Distribution of surface fluorescence intensity values after application of cell-impermeable dye in transfected cells for FAP-BK $\alpha$  (red bars) or FAP-BK $\alpha$ + $\beta$ 4 (black bars). (H-I) Proposed model for surface distribution of BK channels in the absence (H) or presence (I) of the  $\beta$ 4 subunit. doi:10.1371/journal.pone.0033429.g001

highest intensity, and distance was normalized to the maximum distance for that cell. The normalized values across all cells were averaged and plotted as shown in Figure 2.

### Electrophysiology

All electrophysiological experiments were performed as previously described [7]. The  $\beta$ 4 knock-out mice used in these studies were inbred 5 generations to Jackson Labs C57BL/6J mice.  $\beta$ 4 knock-out animals in the C57BL/6J genetic background were studied with EEG recordings and found to lack seizures (in contrast to the mixed 129/B6 background used in Brenner et al., 2005). In short, brains from P13–P15 C57BL/6 or  $\beta$ 4 knock-out

mice on a C57BL/6 background mice were sectioned coronally at 300  $\mu$ m in a solution composed of (in mM): 110 choline chloride, 2.5KCl, 7 MgCl<sub>2</sub>, 1 NaH<sub>2</sub>PO<sub>4</sub>, 26.2 NaHCO<sub>3</sub>, 0.5CaCl<sub>2</sub>, 25 glucose, 11.6 sodium ascorbate and 3.1 sodium pyruvate. Slices were recovered in artificial cerebrospinal fluid (ACSF) composed of (in mM): 119 NaCl, 2.5 KCl, 1.3 MgSO<sub>4</sub>, 2.5 CaCl<sub>2</sub>, 1 NaH<sub>2</sub>PO<sub>4</sub>, 26.2 NaHCO<sub>3</sub>, 11 glucose equilibrated with 95/5% O<sub>2</sub>/CO<sub>2</sub> at 34°C for 20 minutes and then maintained at room temperature. Recordings were performed at room temperature. Somata of CA3 pyramidal neurons in the hippocampus were targeted for whole-cell recording at room temperature with borosilicate glass electrodes with a resistance of 4–8 M $\Omega$ .

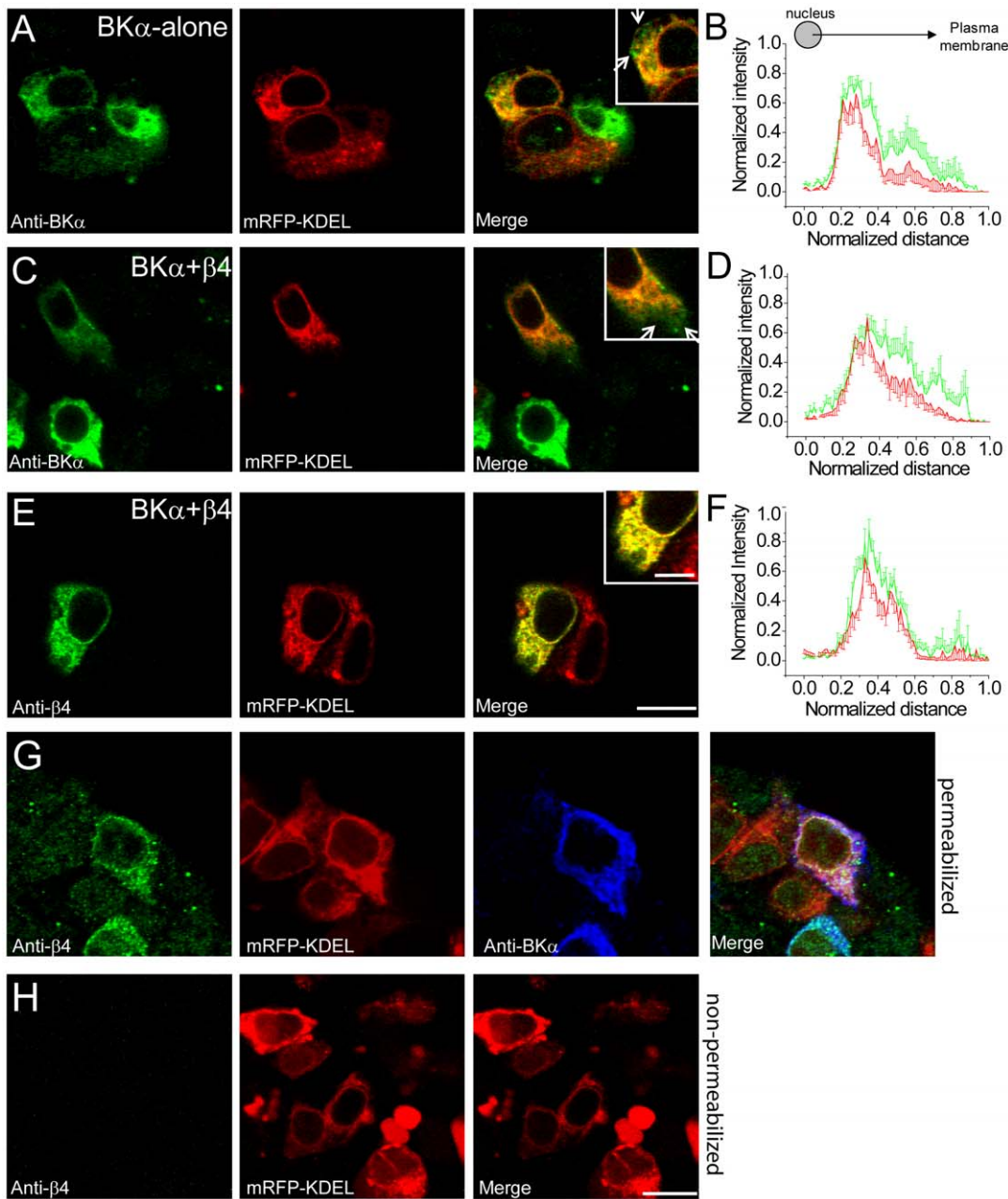


**Figure 2. Immunofluorescence reveals that BK $\alpha$  and  $\beta$ 4 are substantially localized to the ER and that  $\beta$ 4 is difficult to detect on the cell surface.** (A) Immunocytochemistry against fixed, permeabilized HEK-293 cells for the FAP-BK $\alpha$  subunit (anti-BK $\alpha$ : green) and the ER-marker mRFP-KDEL (intrinsic fluorescence; red) in cells transfected with BK $\alpha$  alone. Inset shows a cell with overlapping expression of BK $\alpha$  and mRFP-KDEL with arrows pointing to regions containing only BK $\alpha$ . (B) Quantitation of normalized intensity versus normalized distance from the cell nucleus for anti-BK $\alpha$  (green) and mRFP (red) in transfected cells. (C) As in (A) but for cells expressing BK $\alpha$  (green),  $\beta$ 4 (unlabeled; not visualized) and mRFP-KDEL (red). (D) Same as (B) but in cells expressing BK $\alpha$ ,  $\beta$ 4 and mRFP-KDEL. (E) Localization of the  $\beta$ 4 subunit (anti- $\beta$ 4: green) and mRFP-KDEL (intrinsic fluorescence; red) in cells expressing BK $\alpha$  (unlabeled; not visualized),  $\beta$ 4 and mRFP-KDEL. Scale bar = 20  $\mu$ m or 5  $\mu$ m for inset. (F) As in (B), but for  $\beta$ 4 and mRFP-KDEL. (G) Localization of the  $\beta$ 4 subunit (anti- $\beta$ 4: green), mRFP-KDEL (intrinsic fluorescence; red) and BK $\alpha$  (anti- $\alpha$ : blue) in transfected, fixed HEK-293 cells expressing BK $\alpha$ ,  $\beta$ 4, and mRFP-KDEL. (H) Expression pattern of the  $\beta$ 4 subunit (anti- $\beta$ 4: green) and mRFP-KDEL (intrinsic fluorescence; red) under non-permeabilized immunohistochemistry conditions. Note that immunohistochemical detection of cell-surface BK $\alpha$  is difficult because of an intracellular epitope for BK $\alpha$ . Scale bar = 10  $\mu$ m (G,H).  
 doi:10.1371/journal.pone.0033429.g002

Electrode internal solution was composed of (in mM): 116 potassium gluconate, 6 KCl, 8 NaCl, 4 MgATP, and 0.4 NaGTP, at pH 7.25–7.35, 290 mOsm. Free calcium was unbuffered to allow calcium accumulation during depolarization steps. Paxilline (Pax; 10 nM or 1  $\mu$ m; Sigma) and Iberiotoxin (Ibt; 50 nM;

Sigma) were bath applied for at least 10 minutes to saturate channel block before further measurements.

To estimate the magnitude of steady-state BK channel currents in CA3 neurons, cells were held at  $-80$  mV and a 40 ms prepulse of  $-40$  mV followed by an 800 ms voltage step to  $+100$  mV was

applied before and after the application of paxilline or iberiotoxin. Currents from after drug application were subtracted from the pre-application currents to yield the paxilline-sensitive or iberiotoxin-sensitive BK channel current. The current from the voltage step was determined from an average of 4 sweeps. Capacitive current was subtracted for both the pre- and post-drug application currents by the P/4 method.

In comparison to recordings from heterologous cells, estimating BK channel currents in neurons is considerably more difficult. We are aware that our measurements may be dominated by BK channels that lie close to the soma, due to inadequate voltage clamp in the distal portions of the cell. However, because the critical comparisons for this study were of the steady-state currents isolated by two different drugs, and all other recording parameters were the same (cell type, cell age, input resistance), we expect that these uncontrolled variables should cancel out.

## Results

### $\beta 4$ exerts a dominant negative effect on cell-surface trafficking of BK channels

Tracking the surface distribution of ion channels, a technically challenging issue in cellular neuroscience, has long been a subject of great interest. Although intrinsically fluorescent protein tags such as synaptophysin have been used to examine surface expression of other membrane proteins, intracellular fluorescence is incompletely quenched at near-neutral pH in some intracellular compartments such as the ER [34]. Since many ion channels show enormous intracellular reservoirs, this fluorescence makes it difficult to resolve or quantitate lower levels of cell-surface staining. To bypass this, a FAP [33] was used to genetically tag the  $\alpha$  subunit of the BK channel at the extracellular N-terminus [35] (Figure 1A). Upon small-molecule dye binding to the FAP, fluorescent output is enhanced 20,000-fold, providing outstanding signal-to-noise (Figure 1B). Because well-characterized antibodies against extracellular regions of BK $\alpha$  have not been generated, FAP-tagging of the protein enabled direct comparison of cell-surface channel localization using a cell-impermeable dye, malachite green diethylene glycol (MG-2p; [33]), in the presence and absence of  $\beta 4$ . Furthermore, this analysis could be carried out in living cells under normal growth and temperature conditions. This is particularly important, because channel trafficking can be acutely altered by temperature and mechanical stress [29,30,36].

The genes encoding BK $\alpha$  and  $\beta 4$  were isolated from mouse brain tissue, and cloned into a mammalian expression vector. Sequences matched the BK $\alpha$  STREX-lacking isoform [37] and the canonical  $\beta 4$  transcript (Figures S1, S2). The L5 FAP tag was fused in frame to the N-terminus of BK $\alpha$ , at the amino acid sequence beginning MDALIIIPV. In HEK-293 cells transfected with FAP-tagged BK $\alpha$  alone, application of the impermeable MG-2p dye revealed a clear outline of the plasma membrane (Figure 1C). Cotransfection of FAP-BK $\alpha$  with unlabeled  $\beta 4$  revealed a marked reduction in cell-surface fluorescence in the presence of MG-2p dye (Figure 1D). This was not due to suppression of BK $\alpha$ -protein in cotransfected cells, since application of a membrane-permeable MG-ester dye revealed FAP-BK $\alpha$  in intracellular compartments under both transfection conditions (Figure 1E, F).

Quantitative analysis of cell-surface fluorescence was carried out for FAP-BK $\alpha$ -alone and FAP-BK $\alpha$ + $\beta 4$  transfected cells. Because HEK-293 cells can show a range of values for surface fluorescence, a phenomenon that is likely to depend upon different levels of gene expression in the transfected cells, a histogram was constructed for fluorescence values across multiple cells for each transfection

condition. A significant difference in the across-cell distribution of fluorescence intensity was observed for the two experimental groups (Figure 1G;  $n=54$  regions of interest (ROIs) for each condition, averaged over five independent transfections, 270 ROIs total,  $p<10^{-3}$  by two-sample K-S test). Overall, the presence of  $\beta 4$  induced a nearly 70% reduction in mean surface fluorescence (normalized mean surface intensity, FAP-BK $\alpha$ -alone,  $1\pm 0.03$ , versus FAP-BK $\alpha$ + $\beta 4$ ,  $0.34\pm 0.02$ ,  $p<10^{-5}$  by paired t-test; see also Figure 3). Similar intracellular but different cell-surface expression of BK $\alpha$  in the absence/presence of  $\beta 4$  are schematized in Figure 1H,I.

As an additional method to evaluate  $\beta 4$ -regulated surface expression of BK $\alpha$ , dual-label immunohistochemistry on transfected, fixed HEK-293 cells was performed and analyzed by confocal microscopy of a thin z-section through the cell (Figure S3). These experiments took advantage of small differences in the level of  $\beta 4$  expression in different transfected cells and allowed comparison of surface to internal BK $\alpha$  on a cell-by-cell basis. Surface BK $\alpha$  was tightly coupled to the amount of  $\beta 4$  expressed, with cells expressing little  $\beta 4$  showing the greatest surface:internal ratio. Conversely, cells that expressed high levels of  $\beta 4$  exhibited

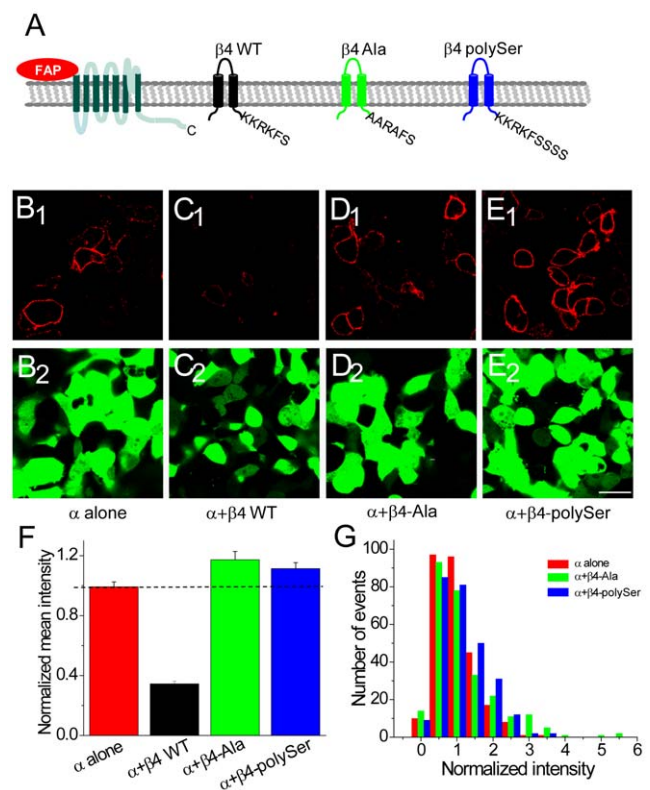


**Figure 3. An ER-retention/retrieval sequence at the C-terminus of  $\beta 4$  inhibits the surface expression of BK $\alpha$  and  $\beta 4$ .** (A) Schematic of the mutant  $\beta 4$  constructs showing the C-terminal amino acids. (B) Fluorescence from binding of cell-impermeable dye to cell-surface BK $\alpha$  channels in cells transfected with FAP-BK $\alpha$  (red) and GFP (green). (C) Same as (B) but in cells transfected with FAP-BK $\alpha$  and wild-type  $\beta 4$ . (D) Same as (B) but in cells transfected with FAP-BK $\alpha$  and  $\beta 4$ -Ala. (E) Same as (B) but in cells transfected with FAP-BK $\alpha$  and  $\beta 4$ -polySer. Scale bar=20  $\mu$ m (B–E). (F) Mean intensity of surface fluorescence for  $\beta 4$  constructs normalized to fluorescence from cells transfected with FAP-BK $\alpha$  alone. (G) Histogram showing distribution of fluorescence intensity in cells transfected with FAP-BK $\alpha$  alone (red), FAP-BK $\alpha$ + $\beta 4$ -Ala (green) and FAP-BK $\alpha$ + $\beta 4$ -polySer (blue). Scale bar: 20  $\mu$ m (B–E).

doi:10.1371/journal.pone.0033429.g003

the lowest ratio of surface: internal BK $\alpha$  immunofluorescence (Figure S3A–F). This conclusion was further supported by live cell imaging experiments using spectrally-distinct cell-permeable and impermeable dyes. In BK $\alpha$ + $\beta$ 4 transfected cells, surface labeling of the FAP-tagged BK $\alpha$  was notably lower compared to the BK $\alpha$ -alone although intracellular levels of BK $\alpha$  appeared grossly similar (data not shown).

### $\beta$ 4 concentrates BK channels in the ER

$\beta$ 4 expression might reduce surface BK $\alpha$  levels by facilitating degradation of the pore-forming channel, or by interacting with BK $\alpha$  subunits to reduce cell-surface trafficking. To determine whether BK $\alpha$  and  $\beta$ 4 are concentrated in the same intracellular compartment and to identify this structure, HEK-293 cells were co-transfected with FAP-BK $\alpha$ ,  $\beta$ 4, and monomeric RFP (mRFP) tagged with an N-terminal prolactin signal sequence and a C-terminal sequence (KDEL) that leads to protein retention in the endoplasmic reticulum (ER; mRFP-KDEL; gift of T. Lee and E.L. Snapp; [38]). Importantly, untransfected HEK-293 cells exhibited no BK $\alpha$  or  $\beta$ 4 immunoreactivity, indicating that these cells do not express endogenous BK channel subunits that might alter trafficking results [39] (and data not shown).

In FAP-BK $\alpha$  and mRFP-KDEL transfected and fixed cells, clear colocalization of immunolabeled BK $\alpha$  and mRFP was observed, indicating that the bulk of BK $\alpha$  subunits reside in the ER (Figure 2A). This is similar to what has been observed for other K<sup>+</sup> channel proteins that also show large intracellular reserves [40,41,42]. By immunohistochemistry, BK $\alpha$  signal was not pronounced at the margins of the cell, highlighting the benefits of the FAP tag that allows visualization of cell-surface protein without spectral contamination from intracellular stores.

In FAP-BK $\alpha$ + $\beta$ 4-expressing cells, BK $\alpha$  immunolabeling showed similar overlap with mRFP-KDEL (Figure 2C). However, in both FAP-BK $\alpha$ -alone and  $\beta$ 4 cotransfected cells, some BK $\alpha$  could be observed outside of the mRFP-KDEL ER compartment, indicating that at least some fraction of the BK $\alpha$  subunit may escape the ER (Figure 2B,D; both distributions are significantly different,  $p < 0.001$  by K-S test).

$\beta$ 4 immunostaining in fixed transfected cells confirmed both  $\beta$ 4 subunit expression and  $\beta$ 4 colocalization with BK $\alpha$  and KDEL-mRFP (Figure 2E–G). Localization analysis indicated that  $\beta$ 4 and mRFP-KDEL distributions were not significantly different (Figure 2F,  $p > 0.1$ ), suggesting that the  $\beta$ 4 subunit is largely retained within the ER. Based upon the finding that  $\beta$ 4 co-expression is sufficient to reduce surface FAP-BK $\alpha$ , as well as that immunofluorescence for both proteins show substantial overlap with mRFP-KDEL and with each other, we propose that  $\beta$ 4 directly interacts with the BK $\alpha$  subunit to retain the channel complex in the ER.

Since the epitope for the  $\beta$ 4 antibody is within the extracellular loop of the two-transmembrane domain protein (see Figure 1A), surface localization of  $\beta$ 4 can be determined by immunocytochemistry in non-permeabilized cells. Under these conditions,  $\beta$ 4 immunoreactivity was not observed at the cell surface (Figure 2H) even though significant  $\beta$ 4 expression can be seen after permeabilization (Figure 2G). These data show that although transfected HEK-293 cells indeed express  $\beta$ 4 protein, this  $\beta$ 4 protein is undetectable at the plasma membrane.

### Identification of an ER retention motif in $\beta$ 4

The amino acid determinants of proteins that reside in the ER have been well-defined [41,43,44,45]. Canonical amino acid motifs for ER retention/retrieval of both luminal and transmembrane proteins are KDEL or KKXX at the carboxy (C)-terminus

(where XX are the last two amino acids of the protein) respectively. Although  $\beta$ 4 lacks either of these canonical motifs, the last six amino acids, KKRRKFS, may also serve as an ER retention sequence under some conditions [44] (Figure 3A).

To test whether these amino acid residues in  $\beta$ 4 were sufficient to exclude co-expressed FAP-tagged BK $\alpha$  from the plasma membrane, these lysine residues were mutated to alanines ( $\beta$ 4-Ala; Figures 3A, S2). Because it has also been demonstrated that the KKXX motif must be at the C-terminus of the protein [44], we also investigated whether addition of three amino acids (serines) to the C-terminus would disrupt the ER retention/retrieval function of  $\beta$ 4 ( $\beta$ 4-polySer; Figures 3A, S2).

Cotransfection of FAP-BK $\alpha$  with  $\beta$ 4-Ala or FAP-BK $\alpha$  with  $\beta$ 4-polySer, followed by application of the impermeable MG-2p dye, exhibited robust surface fluorescence for both co-transfected  $\beta$ 4 mutants (Figure 3B–E). Quantitation of surface fluorescence intensity across cells indicated that mean surface fluorescence was similar or even greater than FAP-BK $\alpha$ -only transfected cells (normalized mean surface intensity:  $\beta$ 4-Ala  $1.17 \pm 0.06$ ,  $\beta$ 4-polySer  $1.12 \pm 0.04$ ; significantly different from BK $\alpha$ -alone by ANOVA;  $n = 54$  ROIs per transfection experiment over 5 experiments total for each mutant; Figure 3F). In addition, the distribution of FAP-BK $\alpha$  fluorescence surface intensity values for the two mutant  $\beta$ 4 proteins was fully overlapping with that observed for FAP-BK $\alpha$ -alone transfected cells ( $p = 0.10$  by two-sample K-S test for  $\beta$ 4-Ala and  $p = 0.13$  for  $\beta$ 4-polyser versus BK $\alpha$  alone; Figure 3G). Thus, the  $\beta$ 4 C-terminal motif KKRRKFS is required for ER retention of the BK $\alpha$  channel subunit in transfected HEK-293 cells.

An alternate explanation for the increased surface localization of BK $\alpha$  is that mutant  $\beta$ 4 constructs are not efficiently expressed in transfected cells. To verify that the  $\beta$ 4-Ala and  $\beta$ 4-polySer constructs are present in cells expressing BK $\alpha$ ,  $\beta$ 4-immunocytochemistry was carried out in the FAP-BK $\alpha$  and mutant  $\beta$ 4 transfected HEK-293 cells. Strong intracellular immunoreactivity for both  $\beta$ 4-Ala (Figure 4A) and  $\beta$ 4-polySer was observed, indicating that these mutations do not markedly suppress  $\beta$ 4 protein levels.

Immunocytochemistry using a  $\beta$ 4 antibody in non-permeabilized cells revealed robust cell-surface staining for both  $\beta$ 4-Ala and  $\beta$ 4-polySer cotransfections with FAP-BK $\alpha$  (Figure 4B,D). This demonstrates that our experimental conditions are sufficient to detect not just FAP-tagged BK $\alpha$ , but also  $\beta$ 4 protein, at the cell surface. The presence of both FAP-tagged BK $\alpha$  and mutant  $\beta$ 4 at the cell surface suggest that modifications of the C-terminal sequence of  $\beta$ 4 are sufficient to liberate BK $\alpha$ + $\beta$ 4 channels from the ER.

### $\beta$ 4-containing channels have a minor contribution to whole-cell BK channel currents in hippocampal neurons

Although many trafficking studies are carried out in heterologous cells, protein overexpression may alter steady-state distributions of channels. A more appropriate test of whether  $\beta$ 4-containing BK channels are present and functional at the cell surface is to examine BK channel properties in CNS neurons that endogenously express high levels of  $\beta$ 4. Because the majority of BK channels in neurons, as in HEK-293 cells, reside in intracellular stores [46], cell-surface immunolocalization of BK channels in brain tissue is difficult to resolve. However, BK channel currents can be electrophysiologically isolated using whole-cell patch clamp recording, a direct method to analyze BK channel function in living neurons.

To identify brain areas that express elevated  $\beta$ 4 in control tissue, *in situ* hybridization using a  $\beta$ 4 anti-sense probe was performed. Hybridization in hippocampal area CA3 was substantially greater

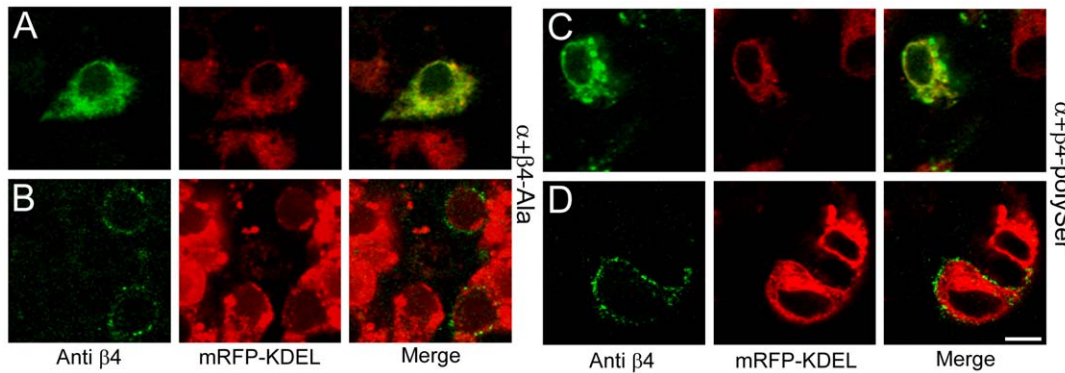


**Figure 4. Mutation of the C-terminal ER-retention/retrieval sequence in  $\beta 4$  liberates  $\beta 4$  to the surface.** (A) Expression pattern of the cotransfected FAP-BK $\alpha$  (unlabeled; not visualized),  $\beta 4$ -Ala mutant (anti- $\beta 4$  immunocytochemistry: green) and mRFP- KDEL (intrinsic fluorescence; red) in fixed, permeabilized HEK-293 cells. (B) Same as (A) but under non-permeabilized conditions. (C) Same as for (A) but for  $\beta 4$ -polySer mutant under permeabilized conditions. (D) Same as (C) but under non-permeabilized conditions. Scale bar = 10  $\mu$ m (A–D). doi:10.1371/journal.pone.0033429.g004

than in almost any other brain area (Figure 5A, B). If  $\beta 4$ -containing BK channels at the cell-surface play a major role in regulating neuronal BK currents, we reasoned that this would be prominent in these neurons.

To probe for the presence of BK $\alpha$ + $\beta 4$ -containing channels, whole-cell patch-clamp recordings from CA3 pyramidal neurons were carried out and BK channel currents were identified using a pharmacological subtraction method (Figure 5E). The pan-BK antagonist paxilline, which blocks all BK channels, was used to isolate the whole-cell BK current, and this value was compared to the amplitude of the iberiotoxin-sensitive current. If the majority of current is carried by BK $\alpha$ + $\beta 4$  channels, we reasoned that the amplitude of the iberiotoxin-sensitive current would be significantly smaller than the paxilline-sensitive current (schematized in Figure 5F). Alternatively, if there was little or no current carried by BK $\alpha$ + $\beta 4$  channels, there should be no difference between the amplitude of the paxilline-sensitive and the iberiotoxin-sensitive current (schematized in Figure 5G).

Whole-cell K<sup>+</sup> currents were isolated before and after antagonist application and subtracted offline. Because  $\beta 4$ -containing channels are slowly activating and may take hundreds of milliseconds to reach peak current [20,21,23], current amplitude was calculated at the end of an 800 ms pulse from  $-80$  to  $+100$  mV (Figure 5H–J).

Using the pan-BK channel antagonist paxilline, the magnitude of steady-state BK channel current was  $1.40 \pm 0.22$  nA (10 nM paxilline;  $n = 7$  cells; Figure 5H). Although these experiments typically used a concentration of paxilline that reflects the low IC<sub>50</sub> established for this drug [47,48], similar current amplitudes were also obtained using drug concentrations that were 100-fold higher (1  $\mu$ M paxilline  $1.35 \pm 0.26$  nA,  $n = 6$  cells;  $p = 0.9$  versus 10 nM paxilline; Figure 5H,J). Thus, it is unlikely that we systematically underestimated the amplitude of BK channel currents.

Surprisingly, the magnitude of iberiotoxin-sensitive BK channel currents was nearly identical to that obtained using the pan-BK channel antagonist paxilline (50 nM iberiotoxin;  $1.59 \pm 0.62$  nA,  $n = 6$  cells;  $p = 0.8$  versus 10 nM paxilline; Figure 5I,J). These data suggest that there is little contribution of  $\beta 4$ -containing BK channels to whole-cell BK channel currents in CA3 pyramidal neurons (Figure 5G). It is alternatively possible that BK channels in CA3 neurons may contain  $\beta 4$  with a reduced stoichiometry that is sensitive to iberiotoxin blockade.

The influence of  $\beta 4$  on the biophysical properties of BK channel currents has been well-studied [1,20,21,22,23,24,25,26,27]. In HEK-293 cells, where voltage clamp can be excellent,  $\beta 4$  typically

slows the activation kinetics ( $\tau$ ) of BK currents [1,20,23,26]. Indeed, these effects of  $\beta 4$  have been postulated to strongly influence channel function in vivo [1]. Estimating  $\tau$  for BK channel currents in neurons is problematic, in part because voltage clamp is imperfect in these cells. Activation time constants for iberiotoxin and paxilline-sensitive currents were comparable ( $\tau = 2.01 \pm 0.56$  ms for 10 nM paxilline;  $2.89 \pm 1.22$  ms for 50 nM iberiotoxin;  $p = 0.29$ ).

Some previous studies, including those where recordings from CNS neurons were carried out, have identified iberiotoxin-resistant BK channel currents. For example, in neurons from the dentate gyrus, single-channel recordings clearly have shown iberiotoxin-resistant BK channels from membrane patches pulled from the cell soma [1]. To resolve this contradiction and determine whether our inability to observe  $\beta 4$ -containing channels might be due to our whole-cell recording approach, we also compared paxilline and iberiotoxin-sensitive whole-cell BK channel currents from dentate gyrus neurons. The magnitude of the iberiotoxin-sensitive current was more than 10-fold smaller than the paxilline-sensitive current (iberiotoxin  $0.11 \pm 0.2$  nA;  $n = 5$  cells versus paxilline  $1.6 \pm 0.06$  nA;  $n = 3$  cells). The activation kinetics of the pharmacologically isolated BK channel current was similar between the iberiotoxin and paxilline-sensitive current, suggesting that this measurement in neurons is an unreliable indicator of the molecular composition of the channel ( $\tau$  for iberiotoxin-sensitive current  $8.41 \pm 1.8$  ms versus paxilline  $7.26 \pm 1.38$  ms). These data show that the pronounced effect that  $\beta 4$  has on BK channel trafficking can be influenced by neuron cell type.

### BK channel currents are larger in $\beta 4$ knock-out animals

A critical test of the hypothesis that  $\beta 4$  can regulate whole-cell BK channel current is to examine the amplitude of BK current in CA3 neurons where no  $\beta 4$  is expressed. Consistent with our in situ hybridization results, hippocampal area CA3 showed strong expression of the GFP reporter that had been knocked-in to the  $\beta 4$  expression locus (Figure 6A). Pharmacological isolation of whole-cell BK channel current revealed that CA3 neurons in  $\beta 4$  knock-out animals showed a highly significant, more than 2.5-fold increase in BK channel current amplitude compared to heterozygote littermates (paxilline-sensitive current in  $\beta 4$  +/- mice:  $1.62 \pm 0.32$  nA;  $n = 11$  cells versus  $\beta 4$  -/- mice  $3.51 \pm 0.59$  nA;  $n = 12$  cells;  $p = 0.01$ , Figure 6C,D). BK channel current amplitude in heterozygote animals was comparable to values from wild-type animals (see Figure 5J).

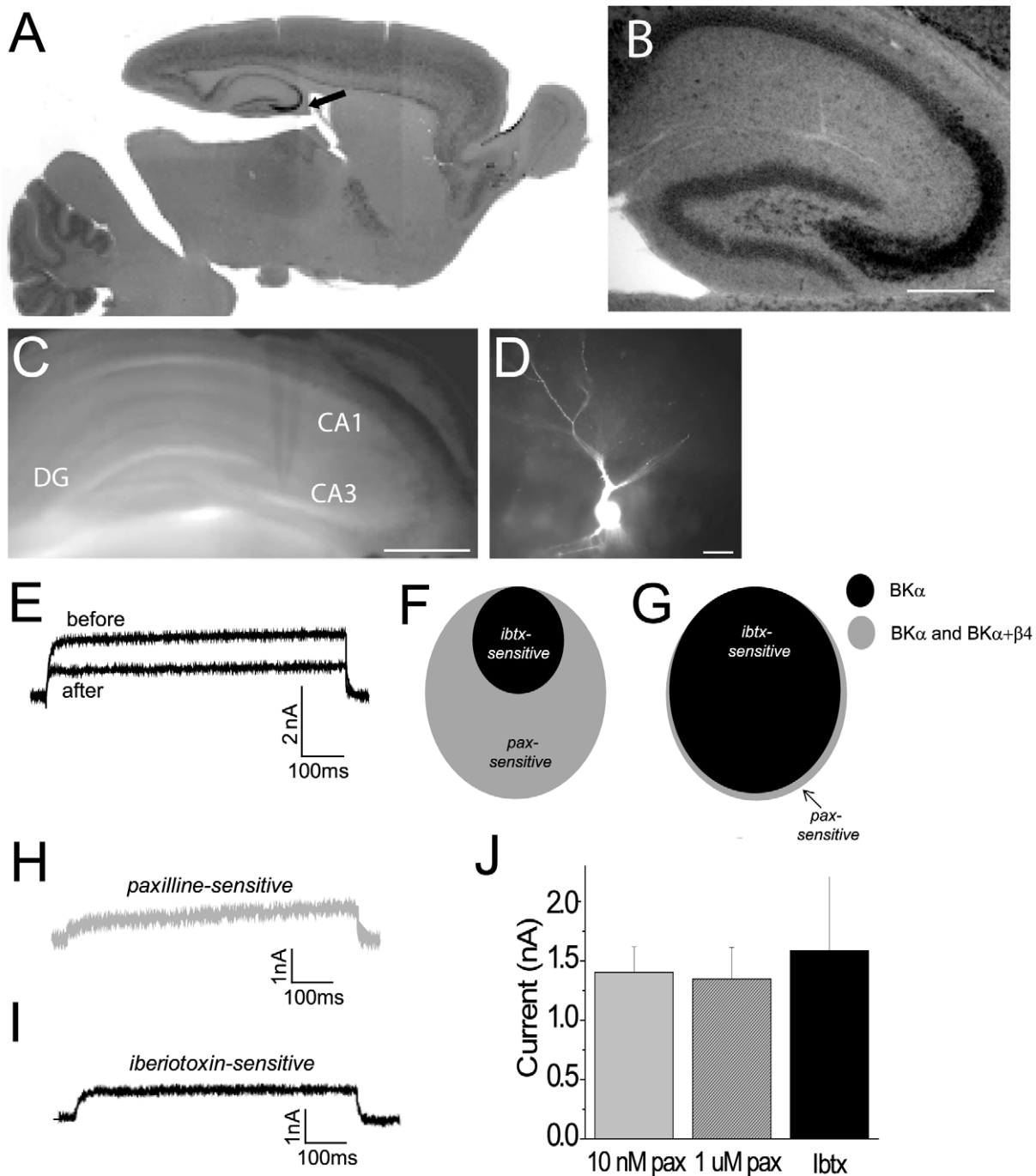


**Figure 5.  $\beta 4$ -containing BK channels do not contribute to whole-cell BK channel currents.** (A) In situ hybridization showing regions of  $\beta 4$  expression in a mouse brain. Arrow points to high levels of expression in the CA3. (B) Hippocampal area CA3 shows robust  $\beta 4$  expression. Scale bar = 200  $\mu\text{m}$ . (C) Bright field image showing a whole cell electrode in the CA3. Scale bar = 500  $\mu\text{m}$ . (D) Fluorescent image of a CA3 pyramidal cell filled with Alexa fluor 568 after whole cell patch clamp recording. Scale bar = 50  $\mu\text{m}$ . (E) Overlaid traces from a representative cell showing total potassium current and the residual potassium current after application of a BK channel blocker. (F) Schematic overlap between paxilline- and iberiotoxin-sensitive currents when  $\beta 4$ -containing BK channels contribute to whole-cell current. (G) Schematic overlap between paxilline- and iberiotoxin-sensitive currents when  $\beta 4$  containing BK channels do not contribute to whole-cell current. (H) Example paxilline-sensitive BK channel current from a representative cell. (I) Example iberiotoxin-sensitive BK channel current from a representative cell. (J) Quantitation of mean paxilline (pax)- and iberiotoxin (ibtx)-sensitive currents from CA3 pyramidal cells. doi:10.1371/journal.pone.0033429.g005

We saw no effect on the activation kinetics for the pharmacologically subtracted currents, which were comparable between the heterozygote and knock-out groups ( $\tau = 2.20 \pm 0.46$  in  $\beta 4 +/ -$  mice versus  $1.61 \pm 0.32$  in  $\beta 4 -/ -$  animals,  $p > 0.1$ ).

These data are in concordance with the negative-regulatory function of  $\beta 4$  on BK channel surface expression that were obtained via live-cell imaging after channel overexpression in heterologous cells.

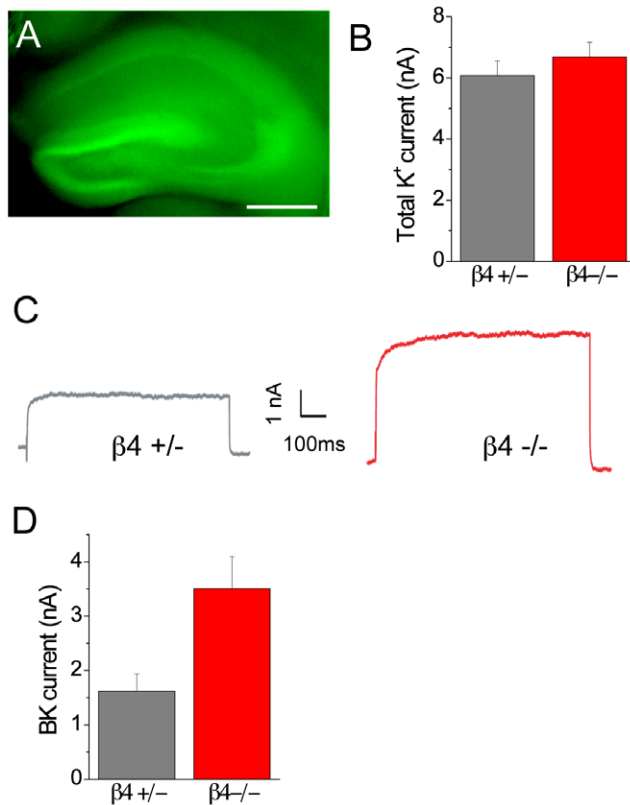


**Figure 6. Genetic ablation of  $\beta 4$  results in larger BK channel currents in CA3 pyramidal neurons.** (A) Fluorescent image of a living slice from a  $\beta 4^{-/-}$  knock-out mouse showing GFP-signal in hippocampus. Scale bar: 500  $\mu\text{m}$ . (B) Mean total potassium current from  $\beta 4$  heterozygote ( $\beta 4^{+/-}$ ) and  $\beta 4$  knock-out ( $\beta 4^{-/-}$ ) mice. (C) Example paxilline-sensitive BK channel current from representative CA3 neurons in  $\beta 4^{+/-}$  and  $\beta 4^{-/-}$  mice. (D) Mean amplitude of paxilline-sensitive BK channel current in  $\beta 4^{+/-}$  and  $\beta 4^{-/-}$  mice. doi:10.1371/journal.pone.0033429.g006

## Discussion

BK channels, because of their large single-channel conductance and co-activation by depolarization and intracellular  $\text{Ca}^{++}$ , play an important role in regulating neuronal firing. BK channels disproportionately contribute to neuronal whole-cell  $\text{K}^{+}$  channel currents, where they can carry more than half the total voltage-gated  $\text{K}^{+}$  current. We have shown that expression of cell-surface BK channels is controlled by the presence of the brain-specific  $\beta 4$  subunit. Using a novel FAP to track the location of tagged BK channels at the cell surface and cytoplasm, we find that coexpression of  $\beta 4$  significantly reduces  $\text{BK}\alpha$  channel protein at the plasma membrane, a function that is dependent upon a C-terminal ER retention/retrieval motif.

In CA3 neurons, which exhibit the highest levels of  $\beta 4$  expression compared to almost any neurons within the rodent CNS, pharmacologically-isolated whole-cell BK channel currents display none of the expected characteristics for  $\text{BK}\alpha + \beta 4$  channels, suggesting that these channels may not be present at the cell surface. Furthermore, genetic ablation of the  $\beta 4$  subunit was sufficient to significantly increase whole-cell BK channel currents in knock-out animals. Thus, we propose that an important function of the CNS-specific BK channel accessory subunit  $\beta 4$  in CA3 neurons is control of cell-surface trafficking of the BK channel complex.

These studies employed a FAP tag to track the location of BK channels in living cells. This methodology has significant advantages compared to more standard techniques, such as GFP protein tags, where the surface fluorescence signal can be overwhelmed by the much larger intracellular stores of channel protein. Although the GFP-based Phluorin [49], a fluorescence protein tag whose signal is quenched in acidic cell compartments, has been useful for studying vesicle fusion [50,51], the nearly neutral pH of the ER has been associated with breakthrough fluorescence that complicates analysis. Advantages of the FAP system are use of membrane permeable and impermeable dyes, high signal-to-noise due to low fluorescence of unbound dye, and the potential to carry out real-time imaging experiments. Since unbound dye has essentially no fluorescence, a specific signal is generated without washing off excess dye, a property that will enable imaging in more complex tissue environments. Additionally, because the fluorescence signal from a single-dye-FAP interaction can be so bright (5 to 20-fold brighter than GFP), this technology may be particularly well-suited to studying the localization and dynamics of individual molecules, such as single BK channels at the plasma membrane.

Much experimental effort has gone into understanding the biophysical consequences of  $\beta 4$  on BK channel function, with little attention to how this auxiliary subunit can control channel localization. Using live-cell imaging and immunolocalization in heterologous cells, as well as electrophysiological measurements in CA3 neurons that express high levels of  $\beta 4$ , we find that  $\beta 4$  expression is associated with a dramatic reduction of BK channels at the cell surface. In addition, we find that genetic ablation of  $\beta 4$  is sufficient to significantly enhance whole-cell BK channel currents. This may explain the paradoxically broad expression of  $\beta 4$  in the CNS (Figure 6 and [20,21,22]) despite iberitoxin-pharmacology indicating that BK channels lack  $\beta 4$  in many neurons [52,53,54,55,56,57]. Taken together, our results suggest that the effect of  $\beta 4$  on channel function may be much more indirect than previously imagined.

Nevertheless, a few studies report the presence of iberitoxin-insensitive BK currents in the CNS, specifically in posterior pituitary nerve terminals and dentate gyrus granule neuronal soma and their mossy fiber terminals [1,2,58,59]. Further, the  $\beta 4$  subunit was found to promote surface expression of the related slo3 channel in *Xenopus* oocytes [60]. How can the present findings be resolved with this? Our comparison of iberitoxin and paxilline-sensitive currents in dentate gyrus neurons indicates that in some neurons,  $\beta 4$  is not sufficient to reduce cell-surface channel expression. Thus, there may be additional factors, including activation of signaling pathways, which can regulate channel localization in a cell-type specific manner.

Some studies have also suggested that the  $\beta 4$  subunit may regulate subcellular distribution of the BK channels into axonal or dendritic compartments [6,59,61,62]. Because of the limitations of voltage clamp in neurons (i.e. poor voltage control in the distal processes of the cell), such  $\beta 4$ -containing channels might be hard to detect in CA3 neurons. It is also possible that BK channels can be redistributed to the plasma membrane under some circumstances, for example, following mechanical dissociation of cells prior to analysis [36,62,63,64], or during periods of high firing. Redistribution could occur over very short time intervals (100 s of ms), during firing bursts, or might be regulated over the course of many minutes. Such regulation has been observed for  $\text{K}_{v}2.1$  type  $\text{K}^{+}$  channels [46]. Our finding that  $\beta 4$  expression is associated with the regulation of surface levels of BK channels suggests a new mechanism for dynamic control of channel activity.

A caveat of the present study is that direct association of the  $\text{BK}\alpha$  subunit with  $\beta 4$  was not directly demonstrated in transfected

cells. However, the rescue of surface expression with co-transfection of the  $\beta 4$  mutant construct suggests that there is some interaction between the two proteins. Furthermore, our preliminary recordings from transfected HEK-293 cells indicate that the increase in surface expression observed in BK $\alpha$ + $\beta 4$ -Ala expressing cells is linked to iberiotoxin-resistant whole-cell currents. Further studies will be required to unambiguously demonstrate the interaction of BK $\alpha$  and  $\beta 4$  in our experimental preparation.

Enhanced BK channel currents have been linked to neuronal hyperexcitability and epilepsy in cortical neurons [1,7,9,65]. Indeed, BK channel antagonists can reduce bursting in abnormally active tissue [4,7] and have a profound anticonvulsant effect *in vivo* [10]. The large contribution of BK channels to the total K<sup>+</sup> channel current in CA3 neurons suggests that these channels may play a particularly important role in controlling the excitability of these cells.

The data presented here characterize the detailed molecular mechanisms that control cellular BK channel trafficking. We have identified a new role for the BK  $\beta 4$  channel subunit – ER retention – as well as the specific amino acid residues that are necessary to direct this function. Additionally, we have shown that BK channels in CA3 neurons are not associated with the pharmacological and biophysical hallmarks of  $\beta 4$ -containing channels as described in previous studies using heterologous cells, and that the absence of  $\beta 4$  is sufficient to significantly enhance whole-cell BK channel current. Because these studies were carried out in CNS neurons in acute brain slices, these findings may be particularly relevant to channel function *in vivo*. The dynamic regulation of endogenous BK channel localization in neurons is an exciting avenue for future investigations.

## Supporting Information

**Figure S1 Sequence of BK $\alpha$  and FAP L5.** (A) Sequence of BK $\alpha$ ; upper case letters in green: Start codon; Upper case letters in red: Stop codon; Bold italicized text: Exon start site; Bold text in red: ALCOREX/exon 24; Black arrows show position of primers

## References

- Brenner R, Chen QH, Vilaythong A, Toney GM, Noebels JL, et al. (2005) BK channel beta4 subunit reduces dentate gyrus excitability and protects against temporal lobe seizures. *Nat Neurosci* 8: 1752–1759.
- Dopico AM, Widmer H, Wang G, Lemos JR, Treisman SN (1999) Rat supraoptic magnocellular neurones show distinct large conductance, Ca<sup>2+</sup>-activated K<sup>+</sup> channel subtypes in cell bodies versus nerve endings. *J Physiol* 519 Pt 1: 101–114.
- Gu N, Vervaeke K, Storm JF (2007) BK potassium channels facilitate high-frequency firing and cause early spike frequency adaptation in rat CA1 hippocampal pyramidal cells. *J Physiol* 580: 859–882.
- Jin W, Sugaya A, Tsuda T, Ohguchi H, Sugaya E (2000) Relationship between large conductance calcium-activated potassium channel and bursting activity. *Brain Res* 860: 21–28.
- Meredith AL, Wiler SW, Miller BH, Takahashi JS, Fodor AA, et al. (2006) BK calcium-activated potassium channels regulate circadian behavioral rhythms and pacemaker output. *Nat Neurosci* 9: 1041–1049.
- Raffaelli G, Saviane C, Mohajerani MH, Pedarzani P, Cherubini E (2004) BK potassium channels control transmitter release at CA3-CA3 synapses in the rat hippocampus. *J Physiol* 557: 147–157.
- Shruti S, Clem RL, Barth AL (2008) A seizure-induced gain-of-function in BK channels is associated with elevated firing activity in neocortical pyramidal neurons. *Neurobiol Dis* 30: 323–330.
- Du W, Bautista JF, Yang H, Diez-Sampedro A, You SA, et al. (2005) Calcium-sensitive potassium channelopathy in human epilepsy and paroxysmal movement disorder. *Nat Genet* 37: 733–738.
- Wang B, Rothberg BS, Brenner R (2009) Mechanism of increased BK channel activation from a channel mutation that causes epilepsy. *J Gen Physiol* 133: 283–294.
- Sheehan JJ, Benedetti BL, Barth AL (2009) Anticonvulsant effects of the BK-channel antagonist paxilline. *Epilepsia* 50: 711–720.
- Ghezzi A, Pohl JB, Wang Y, Atkinson NS (2010) BK channels play a counter-adaptive role in drug tolerance and dependence. *Proc Natl Acad Sci U S A* 107: 16360–16365.
- Bekisz M, Garkun Y, Wabno J, Hess G, Wrobel A, et al. (2010) Increased excitability of cortical neurons induced by associative learning: an *ex vivo* study. *Eur J Neurosci* 32: 1715–1725.
- Matthews EA, Disterhoft JF (2009) Blocking the BK channel impedes acquisition of trace eyeblink conditioning. *Learn Mem* 16: 106–109.
- Nelson AB, Krispel CM, Sekirnjak C, du Lac S (2003) Long-lasting increases in intrinsic excitability triggered by inhibition. *Neuron* 40: 609–620.
- Quirk JC, Reinhard PH (2001) Identification of a novel tetramerization domain in large conductance K(ca) channels. *Neuron* 32: 13–23.
- Shen KZ, Lagrutta A, Davies NW, Standen NB, Adelman JP, et al. (1994) Tetraethylammonium block of Slowpoke calcium-activated potassium channels expressed in *Xenopus* oocytes: evidence for tetrameric channel formation. *Pflugers Arch* 426: 440–445.
- Knaus HG, Garcia-Calvo M, Kaczorowski GJ, Garcia ML (1994) Subunit composition of the high conductance calcium-activated potassium channel from smooth muscle, a representative of the mSlo and slowpoke family of potassium channels. *J Biol Chem* 269: 3921–3924.
- Wang YW, Ding JP, Xia XM, Lingle CJ (2002) Consequences of the stoichiometry of Slo1 alpha and auxiliary beta subunits on functional properties of large-conductance Ca<sup>2+</sup>-activated K<sup>+</sup> channels. *J Neurosci* 22: 1550–1561.
- Torres YP, Morera EJ, Carvacho I, Latorre R (2007) A marriage of convenience: beta-subunits and voltage-dependent K<sup>+</sup> channels. *J Biol Chem* 282: 24485–24489.
- Brenner R, Jegla TJ, Wickenden A, Liu Y, Aldrich RW (2000) Cloning and functional characterization of novel large conductance calcium-activated potassium channel beta subunits, hKCNMB3 and hKCNMB4. *J Biol Chem* 275: 6453–6461.
- Weiger TM, Holmqvist MH, Levitan IB, Clark FT, Sprague S, et al. (2000) A novel nervous system beta subunit that downregulates human large conductance calcium-dependent potassium channels. *J Neurosci* 20: 3563–3570.
- Behrens R, Nolting A, Reimann F, Schwarz M, Waldschutz R, et al. (2000) hKCNMB3 and hKCNMB4, cloning and characterization of two members of

used in cloning BK $\alpha$ . (B) DNA sequence of FAP L5. (C) Amino acid sequence of FAP L5. The L91S mutation is in red. (TIF)

**Figure S2 Sequence of wild-type and mutant  $\beta 4$ .** Bold text in red: Changes from wild type  $\beta 4$  sequence. Black arrows show position of primers used in cloning  $\beta 4$ . (TIF)

**Figure S3  $\beta 4$  reduces surface expression of BK channel  $\alpha$  subunit.** (A–C) Immunocytochemistry on fixed, permeabilized HEK-293 cell expressing FAP-BK  $\alpha$ + $\beta 4$  subunits. (A) Anti-BK $\alpha$  immunocytochemistry. (B) Anti- $\beta 4$  immunocytochemistry for the same cell. (C) Merge of (A) in red and (B) in green. Scale bar = 10  $\mu$ m (A–C). (D) Zoom of region within the red box in (A). The area within D1 and D2 are example ROIs used to calculate the intensity of surface (D1) and internal (D2) BK $\alpha$  expression, respectively, in a transfected cell. (E) Zoom of region within the red box in (B). The area within E1 is an example ROI used to calculate the intensity of  $\beta 4$  in a transfected cell. Scale bar = 5  $\mu$ m (D–E). (F) Graph shows the mean BK $\alpha$  surface to internal ratio (i.e., D1/D2) to  $\beta 4$  expression (i.e., E1) for individual cells (30 ROIs per cell, n = 31 cells). (TIF)

## Acknowledgments

We thank Jill Guy and Joanne Steinmiller for expert animal care, Crissie Remmers for *in situ* hybridization experiments, and members of the Barth laboratory, Tina Lee and Adam Linstedt for helpful comments on the manuscript.

## Author Contributions

Conceived and designed the experiments: SS JU-C MPB ALB. Performed the experiments: SS JU-C. Analyzed the data: SS JU-C JAF. Contributed reagents/materials/analysis tools: RB MPB ALB. Wrote the paper: SS RB ALB.

- the large-conductance calcium-activated potassium channel beta subunit family. *FEBS Lett* 474: 99–106.
23. Ha TS, Heo MS, Park CS (2004) Functional effects of auxiliary beta4-subunit on rat large-conductance Ca(2+)-activated K(+) channel. *Biophys J* 86: 2871–2882.
  24. Jin P, Weiger TM, Wu Y, Levitan IB (2002) Phosphorylation-dependent functional coupling of hSlo calcium-dependent potassium channel and its hbeta 4 subunit. *J Biol Chem* 277: 10014–10020.
  25. Lippiat JD, Standen NB, Harrow ID, Phillips SC, Davies NW (2003) Properties of BK(Ca) channels formed by bicistronic expression of hSloalpha and beta1–4 subunits in HEK293 cells. *J Membr Biol* 192: 141–148.
  26. Wang B, Rothberg BS, Brenner R (2006) Mechanism of beta4 subunit modulation of BK channels. *J Gen Physiol* 127: 449–465.
  27. Meera P, Wallner M, Toro L (2000) A neuronal beta subunit (KCNMB4) makes the large conductance, voltage- and Ca2+-activated K+ channel resistant to charybdotoxin and iberiotoxin. *Proc Natl Acad Sci U S A* 97: 5562–5567.
  28. Bai JP, Surguchev A, Navaratnam D (2011) beta4-subunit increases Slo responsiveness to physiological Ca2+ concentrations and together with beta1 reduces surface expression of Slo in hair cells. *Am J Physiol Cell Physiol* 300: C435–446.
  29. Toro B, Cox N, Wilson RJ, Garrido-Sanabria E, Stefani E, et al. (2006) KCNMB1 regulates surface expression of a voltage and Ca2+-activated K+ channel via endocytic trafficking signals. *Neuroscience* 142: 661–669.
  30. Zarei MM, Song M, Wilson RJ, Cox N, Colom LV, et al. (2007) Endocytic trafficking signals in KCNMB2 regulate surface expression of a large conductance voltage and Ca(2+)-activated K+ channel. *Neuroscience* 147: 80–89.
  31. Kang J, Huguenard JR, Prince DA (1996) Development of BK channels in neocortical pyramidal neurons. *J Neurophysiol* 76: 188–198.
  32. Kaufmann WA, Kasugai Y, Ferraguti F, Storm JF (2010) Two distinct pools of large-conductance calcium-activated potassium channels in the somatic plasma membrane of central principal neurons. *Neuroscience* 169: 974–986.
  33. Szent-Gyorgyi C, Schmidt BF, Creeger Y, Fisher GW, Zakel KL, et al. (2008) Fluorogen-activating single-chain antibodies for imaging cell surface proteins. *Nat Biotechnol* 26: 235–240.
  34. Ashby MC, Ibaraki K, Henley JM (2004) It's green outside: tracking cell surface proteins with pH-sensitive GFP. *Trends Neurosci* 27: 257–261.
  35. Wallner M, Meera P, Toro L (1996) Determinant for beta-subunit regulation in high-conductance voltage-activated and Ca(2+)-sensitive K+ channels: an additional transmembrane region at the N terminus. *Proc Natl Acad Sci U S A* 93: 14922–14927.
  36. Hammami S, Willumsen NJ, Olsen HL, Morera FJ, Latorre R, et al. (2009) Cell volume and membrane stretch independently control K+ channel activity. *J Physiol* 587: 2225–2231.
  37. Xie J, McCobb DP (1998) Control of alternative splicing of potassium channels by stress hormones. *Science* 280: 443–446.
  38. Snapp EL, Sharma A, Lippincott-Schwartz J, Hegde RS (2006) Monitoring chaperone engagement of substrates in the endoplasmic reticulum of live cells. *Proc Natl Acad Sci U S A* 103: 6536–6541.
  39. Yu SP, Kerchner GA (1998) Endogenous voltage-gated potassium channels in human embryonic kidney (HEK293) cells. *J Neurosci Res* 52: 612–617.
  40. Hasdemir B, Fitzgerald DJ, Prior IA, Tepikin AV, Burgoyne RD (2005) Traffic of Kv4 K+ channels mediated by KChIP1 is via a novel post-ER vesicular pathway. *J Cell Biol* 171: 459–469.
  41. Ma D, Jan LY (2002) ER transport signals and trafficking of potassium channels and receptors. *Curr Opin Neurobiol* 12: 287–292.
  42. Wang SX, Ikeda M, Guggino WB (2003) The cytoplasmic tail of large conductance, voltage- and Ca2+-activated K+ (MaxiK) channel is necessary for its cell surface expression. *J Biol Chem* 278: 2713–2722.
  43. Itin C, Kappeler F, Linstedt AD, Hauri HP (1995) A novel endocytosis signal related to the KKXX ER-retrieval signal. *Embo J* 14: 2250–2256.
  44. Jackson MR, Nilsson T, Peterson PA (1990) Identification of a consensus motif for retention of transmembrane proteins in the endoplasmic reticulum. *Embo J* 9: 3153–3162.
  45. Shin J, Dunbrack RL, Jr., Lee S, Strominger JL (1991) Signals for retention of transmembrane proteins in the endoplasmic reticulum studied with CD4 truncation mutants. *Proc Natl Acad Sci U S A* 88: 1918–1922.
  46. Misonou H, Mohapatra DP, Park EW, Leung V, Zhen D, et al. (2004) Regulation of ion channel localization and phosphorylation by neuronal activity. *Nat Neurosci* 7: 711–718.
  47. Knaus HG, McManus OB, Lee SH, Schmalhofer WA, Garcia-Calvo M, et al. (1994) Tremorgenic indole alkaloids potentially inhibit smooth muscle high-conductance calcium-activated potassium channels. *Biochemistry* 33: 5819–5828.
  48. Sanchez M, McManus OB (1996) Paxilline inhibition of the alpha-subunit of the high-conductance calcium-activated potassium channel. *Neuropharmacology* 35: 963–968.
  49. Miesenböck G, De Angelis DA, Rothman JE (1998) Visualizing secretion and synaptic transmission with pH-sensitive green fluorescent proteins. *Nature* 394: 192–195.
  50. Bozza T, McGann JP, Mombaerts P, Wachowiak M (2004) In vivo imaging of neuronal activity by targeted expression of a genetically encoded probe in the mouse. *Neuron* 42: 9–21.
  51. Sankaranarayanan S, De Angelis D, Rothman JE, Ryan TA (2000) The use of pHluorins for optical measurements of presynaptic activity. *Biophys J* 79: 2199–2208.
  52. Benhassine N, Berger T (2005) Homogeneous distribution of large-conductance calcium-dependent potassium channels on soma and apical dendrite of rat neocortical layer 5 pyramidal neurons. *Eur J Neurosci* 21: 914–926.
  53. Faber ES, Sah P (2003) Calcium-activated potassium channels: multiple contributions to neuronal function. *Neuroscientist* 9: 181–194.
  54. Hu H, Shao LR, Chavoshy S, Gu N, Trieb M, et al. (2001) Presynaptic Ca2+-activated K+ channels in glutamatergic hippocampal terminals and their role in spike repolarization and regulation of transmitter release. *J Neurosci* 21: 9585–9597.
  55. Isaacson JS, Murphy GJ (2001) Glutamate-mediated extrasynaptic inhibition: direct coupling of NMDA receptors to Ca(2+)-activated K+ channels. *Neuron* 31: 1027–1034.
  56. Smith MR, Nelson AB, Du Lac S (2002) Regulation of firing response gain by calcium-dependent mechanisms in vestibular nucleus neurons. *J Neurophysiol* 87: 2031–2042.
  57. Womack MD, Khodakhah K (2002) Characterization of large conductance Ca2+-activated K+ channels in cerebellar Purkinje neurons. *Eur J Neurosci* 16: 1214–1222.
  58. Alle H, Geiger JR (2007) GABAergic spill-over transmission onto hippocampal mossy fiber boutons. *J Neurosci* 27: 942–950.
  59. Wang G, Thorn P, Lemos JR (1992) A novel large-conductance Ca(2+)-activated potassium channel and current in nerve terminals of the rat neurohypophysis. *J Physiol* 457: 47–74.
  60. Yang CT, Zeng XH, Xia XM, Lingle CJ (2009) Interactions between beta subunits of the KCNMB family and Slo3: beta4 selectively modulates Slo3 expression and function. *PLoS One* 4: e6135.
  61. Misonou H, Menegola M, Buchwalder L, Park EW, Meredith A, et al. (2006) Immunolocalization of the Ca2+-activated K+ channel Slo1 in axons and nerve terminals of mammalian brain and cultured neurons. *J Comp Neurol* 496: 289–302.
  62. Wynne PM, Puig SI, Martin GE, Treisman SN (2009) Compartmentalized {beta} Subunit Distribution Determines Characteristics and Ethanol Sensitivity of Somatic, Dendritic, and Terminal BK Channels in the Rat CNS. *J Pharmacol Exp Ther*.
  63. Bi GQ, Alderton JM, Steinhardt RA (1995) Calcium-regulated exocytosis is required for cell membrane resealing. *J Cell Biol* 131: 1747–1758.
  64. Togo T, Alderton JM, Bi GQ, Steinhardt RA (1999) The mechanism of facilitated cell membrane resealing. *J Cell Sci* 112(Pt 5): 719–731.
  65. Lorenz S, Heils A, Kasper JM, Sander T (2006) Allelic association of a truncation mutation of the KCNMB3 gene with idiopathic generalized epilepsy. *Am J Med Genet B Neuropsychiatr Genet*.